THERMAL ANALYSIS OF AN EYRING-POWELL FLUID-FLOW THROUGH A CONSTRICTED CHANNEL

by

Sufian MUNAWAR [a*] ***and Najma SALEEM*** [b]

[a] Department of Quantitative Methods, College of Business Administration, Imam Abdulrahman Bin Faisal University, Dammam, Saudi Arabia
[b] Department of Mathematics and Natural Sciences, Prince Mohammad Bin Fahd University, Al Khobar, Saudi Arabia

Original scientific paper
https://doi.org/10.2298/TSCI180125308M

This paper is aimed to investigate the entropy generation in a MHD convective flow of Eyring-Powell fluid through a mildly constricted channel. The constriction is assumed to be of regular or irregular shape and is presented inside the channel wall. Mathematical model is developed using the basic laws of conservation of mass, momentum, and energy. The governing equations are normalized using appropriate set of dimensionless variables and solutions are obtained by regular perturbation technique. The solutions are further used to calculate the entropy expression associated with the Second law of thermodynamics. The heat transfer characteristics, like, temperature, isotherms, entropy generation number entropy lines and the Bejan number are analyzed for the variation in magnetic field, shape parameter, and material constants. It is observed that entropy production is maximum in the narrow part of the channel. Moreover, entropy generation rate is higher for the regular parabolic shape as compared to irregular shapes of constriction.

Key words: *entropy generation, magnetic field, constricted channel, eyring powell fluid*

Introduction

The flow through constricted regions is considered as the significant problem in fluid dynamics and thus widely studied by scientists working in mechanical engineering particularly, in physiological fluids. Some well-known examples of constricted channels are venture tubes, weirs, water aspirators, gas stoves, and in biological and biomedical fields, capillaries of the human cardiovascular system, air-flow through the human airways, aortic insufficiency is a chronic heart condition or blood flow through a stenosis. In human body stenosis refers to the tightening and tapering of body passages, such as arteries, orifice, veins, heart valves*, etc.* Such phenomenon is encountered because of accretion of fatty and greasy substances inside the walls of arteries. This blockage disturbs the normal pattern of blood flow. Arteriosclerosis is a common disease which results by the accumulation of cholesterol and fats to form hard structures known as plaques that are holding asymptotic symptoms. Such plaques grow up with the passage of time and make the arteries stiffer and narrower and leads to serious problems such as angina, blood pressure, heart attack, stroke or even death. These plaques may have different shapes and sizes. Some mathematical models of blood flow through stenosis have

* Corresponding author, e-mail: smunawar@iau.edu.sa

been developed in the noteworthy articles [1-5]. Due to the presence of electromagnetic fields in blood flow most of investigators assumed MHD in blood flow problems. In this regards, Sud *et al.* [6] showed that under the appropriate strength of moving magnetic field the flow velocity accelerates. Mekheimer and El Kot [7] examined the effects of magnetic field and Hall current on the physiological flow of micropolar through stenotic artery and concluded that large values of the Hartmann number have increasing effects on impedance and decreasing effects on blood flow velocity. Kumar *et al.* [8] proposed a study dealing with the oscillatory MHD blood flow through an artery carrying mild stenosis and critically studied the effects of magnetic force on different shapes of stenosis.

The study of entropy is extremely useful in biological thermodynamics to understand the flow characteristics at flow transitions such as constricted regions. The break downing of foodstuff in to constituents, and then developing cells, tissues and muscles increase the order in the body and thus reduce entropy. However, the human body convects heat to the environment due to the change in the temperature of the body and the environment. It consumes energy-comprising substances in the form of food and emits heat into space by excreting waste in the form of CO_2, water, urine, and feces. Consequently, the overall entropy of the human body rises. This increase in the entropy of body affects the physiological fluids inside human body such as blood flow, transport of semen, passage of urine from kidney to bladder through ureter, swallowing food through esophagus, transport of lymph in lymphatic vessels*, etc.* Thermodynamically, in a closed system, entropy is produced by various factors. Bejan [9] identified different factors that cause entropy production in four different convective heat transfer configurations. The two major sources of entropy in a convective heat transfer phenomenon, the heat transfer rate and fluid friction, were discovered by Bejan [10]. Readers are referred to a worth reading book by Bejan [11] on the subject for deep understanding of the subject. Afterwards, numerous investigators [12-19] further explored the phenomenon of heat transfer and entropy generation in convective heat flow problems under various physical assumptions. Souidi *et al.* [20] conducted an entropy analysis for a peristaltic pump in a contracting tube. Recently, Munawar *et al.* [21] investigated production of entropy associated with second-law in a biological flow of variable viscosity fluid.

Most of the biological fluids are non-Newtonian fluids in nature. In this regard, Eyring-Powell (EP) fluid [22] gained the importance among scientists because of its accuracy and consistency in calculating the fluid time scale at different polymer concentration. This was used by Yoon and Ghajar [23] to estimate the fluid time scale by experimental shear viscosity measurement. A few recent investigations dealing with EP fluid-flow are mentioned here for the interested readers [24-27]. The flow analysis of EP fluid in a constricted artery has recently been investigated by Saleem and Munawar [28]. Yet there is a room to study the thermodynamical aspects of EP fluid in constricted channel flow. In this study we intended to accomplish this task by investigating the heat transfer and Second law analyses of EP fluid-flow through a constriction of regular/irregular shapes in the presence constant magnetic field. The governing equations of the current convective heat transfer problem are modeled and simplified under mild stenosis assumptions. The solution obtained by Saleem and Munawar [28] is used to solve the energy equation exactly.

Governing equations

Consider a 2-D incompressible flow of EP fluid through a constricted channel as described in [28]. The width of the channel is measured to be $2d_0$. The x-axis is taken along the wall length while y-axis is chosen normal to the wall. A uniform magnetic field of intensity B_0 is applied in the perpendicular direction of the flow assuming small magnetic Reynolds number.

The lower and upper walls of the channel are held at constant temperatures T_1 and T_2, respectively. Mathematically, the shape of constriction due to mild stenosis is given:

$$h'(x') = \begin{cases} d_0\left[1-\eta\left(b^{m-1}(x'-a)-(x'-a)^m\right)\right], & a \le x' \le a+b \\ d_0, & \text{otherwise} \end{cases} \tag{1}$$

for which

$$\eta = \frac{\delta' m^{\frac{m}{m-1}}}{d_0 b^m (m-1)}, \quad m \ne 1 \tag{2}$$

where $h'(x')$ and d_0 represent the channel width with and without stenosis, respectively. The other parameters b, m, and a tell the length, shape and location of stenosis, respectively. Moreover, δ' is maximum height of stenosis which can be reached at position $x' = a + b/m^{1/(m-1)}$, where $m = 2$ corresponds to parabolic shape while other values of m represent irregular shape of stenosis.

Taking viscous dissipation into account the governing equations are given [28]:

$$\rho\left(u'\frac{\partial u'}{\partial x'}+v'\frac{\partial u'}{\partial y'}\right) = -\frac{\partial p'}{\partial x'}+\left(\mu+\frac{1}{\beta C^*}\right)\left(\frac{\partial^2 u'}{\partial x'^2}+\frac{\partial^2 u'}{\partial y'^2}\right)-$$
$$-\frac{1}{2\beta C^{*3}}\left[2\left(\frac{\partial u'}{\partial x'}\right)^2+\left(\frac{\partial u'}{\partial y'}\right)^2+\left(\frac{\partial v'}{\partial x'}\right)^2\right]\left(\frac{\partial^2 u'}{\partial x'^2}+\frac{\partial^2 u'}{\partial y'^2}\right)-\sigma B_0^2 u' \tag{3}$$

$$\rho\left(u'\frac{\partial v'}{\partial x'}+v'\frac{\partial v'}{\partial y'}\right) = -\frac{\partial p'}{\partial y'}+\left(\mu+\frac{1}{\beta C^*}\right)\left(\frac{\partial^2 v'}{\partial x'^2}+\frac{\partial^2 v'}{\partial y'^2}\right)-$$
$$-\frac{1}{2\beta C^{*3}}\left[2\left(\frac{\partial u'}{\partial x'}\right)^2+\left(\frac{\partial u'}{\partial y'}\right)^2+\left(\frac{\partial v'}{\partial x'}\right)^2\right]\left(\frac{\partial^2 v'}{\partial x'^2}+\frac{\partial^2 v'}{\partial y'^2}\right) \tag{4}$$

$$\rho C_P\left(u'\frac{\partial T}{\partial x'}+v'\frac{\partial T}{\partial y'}\right) = k\left(\frac{\partial^2 T}{\partial x'^2}+\frac{\partial^2 T}{\partial y'^2}\right)+\left(\mu+\frac{1}{\beta C^*}\right)\left[\left(\frac{\partial u'}{\partial y'}+\frac{\partial v'}{\partial x'}\right)^2+4\left(\frac{\partial u'}{\partial x'}\right)^2\right]-$$
$$-\frac{2}{3\beta C^{*3}}\left(\frac{\partial u'}{\partial x'}\right)^2\left[2\left(\frac{\partial u'}{\partial x'}\right)^2+2\left(\frac{\partial v'}{\partial y'}\right)^2+\left(\frac{\partial u'}{\partial y'}+\frac{\partial v'}{\partial x'}\right)^2\right]-$$
$$-\frac{1}{3\beta C^{*3}}\left(\frac{\partial u'}{\partial y'}+\frac{\partial v'}{\partial x'}\right)^2\left[\left(\frac{\partial u'}{\partial x'}\right)^2+\left(\frac{\partial v'}{\partial y'}\right)^2+\frac{1}{2}\left(\frac{\partial u'}{\partial y'}+\frac{\partial v'}{\partial x'}\right)^2\right] \tag{5}$$

where p' is the fluid pressure, μ – the coefficient of viscosity, ρ – the density, C_p – the specific heat, k – the thermal conductivity, β – the material constant, and C^* – the fluid time scale parameter.

Introducing the following non-dimensional variables:

$$x=\frac{x'}{b},\ \ y=\frac{y'}{d_0},\ \ u=\frac{u'}{c_0},\ \ v=\frac{bv'}{\delta c_0},\ h=\frac{h'}{d_0},\ \ p=\frac{p'd_0^2}{c_0 b\mu},\ \ \delta=\frac{\delta'}{d_0},\ \ \eta_1=\frac{\delta m^{\frac{m}{m-1}}}{m-1}$$
$$\phi=\frac{a}{b},\ \ B=\frac{1}{\mu\beta C^*},\ \ D=\frac{Bc_0{}^2}{2d_0{}^2 C^{*2}},\ \ \mathrm{M}=\frac{\sigma B_0^2 d_0{}^2}{\mu},\ \ \theta=\frac{T-T_2}{T_1-T_2},\ \ \mathrm{Br}=\frac{\mu c_0{}^2}{k\left(T_1-T_2\right)} \tag{6}$$

where M, ϕ, B, D, and Br represent the Hartmann number, the amplitude ratio, dimensionless material constants for EP fluid model, and the Brinkman number, respectively. Using (6), the governing eqs. (3) and (4) take the form:

$$\frac{\partial p}{\partial x} = (1+B)\frac{\partial^2 u}{\partial y^2} - D\left(\frac{\partial u}{\partial y}\right)^2 \frac{\partial^2 u}{\partial y^2} - \mathrm{M}^2 u \tag{7}$$

which on simplification reduces:

$$(1+B)\frac{\partial^3 u}{\partial y^3} - \frac{D}{3}\frac{\partial}{\partial y}\left[\left(\frac{\partial u}{\partial y}\right)^2 \frac{\partial^2 u}{\partial y^2}\right] - \mathrm{M}^2 \frac{\partial u}{\partial y} = 0 \tag{8}$$

Similarly, eq. (5) gets the following:

$$\frac{\partial^2 \theta}{\partial y^2} + \mathrm{Br}\left\{(1+B)\left(\frac{\partial u}{\partial y}\right)^2 - \frac{D}{3}\left(\frac{\partial u}{\partial y}\right)^4\right\} = 0 \tag{9}$$

Subject to the boundary conditions:

$$\begin{aligned} u &= 0, \quad \theta = 0 \quad \text{at} \quad y = h, \\ u &= 0, \quad \theta = 1 \quad \text{at} \quad y = -h \end{aligned} \tag{10}$$

and eq. (1) gives

$$h = 1 - \eta_1\left[(x-\phi) - (x-\phi)^m\right], \qquad \phi \le x \le \phi + 1 \tag{11}$$

We use the perturbation solution reported in [28] for eqs. (8) and (10), however eq. (9) could be solved exactly using the build-in command *DSolve* of the symbolic computational software MATHEMATICA. The solution expression is not being reported in order to keep simplicity of the script.

Entropy analysis

Following Bejan [10], it is assumed that the entropy in the channel is produced due to major sources, namely, heat transfer and fluid viscous effects. Accordingly, the expression of total volumetric local rate of entropy generation is given:

$$\dot{S}'''_{\mathrm{gen}} = \frac{k}{T_0^2}(\nabla T)^2 + \frac{\mu}{T_0}[\boldsymbol{\tau}\nabla V] \tag{12}$$

After using quantities (6) in eq. (12) and dividing with the characteristic entropy, S_{G0}, we get the total entropy generation number:

$$N_G = \alpha\left(\frac{\partial \theta}{\partial y}\right)^2 + \mathrm{Br}\left\{(1+B)\left(\frac{\partial u}{\partial y}\right)^2 - \frac{D}{3}\left(\frac{\partial u}{\partial y}\right)^4\right\} \tag{13}$$

where α is the dimensionless temperature difference. The average entropy generation number is given:

$$Ns_{\mathrm{avg}} = \frac{1}{\forall}\int_0^x \int_{-h}^{h} N_G \,\mathrm{d}y\mathrm{d}x \tag{14}$$

where $\forall$ is the area of the integrated region. The Bejan number is introduced:

$$\mathrm{Be} = \frac{1}{1+\Phi} \tag{15}$$

and

$$\Phi = \text{Br}\frac{\left\{(1+B)\left(\frac{\partial u}{\partial y}\right)^2 - \frac{D}{3}\left(\frac{\partial u}{\partial y}\right)^4\right\}}{\alpha\left(\frac{\partial \theta}{\partial y}\right)^2} \tag{16}$$

The Bejan number expressed in eq. (15) is bounded between the range 0 to 1. Within this range it exhibits discriminating features of fluid friction *vs.* heat transfer irreversibilities.

Results and discussion

The solutions of problem are used to discuss various heat transfer characteristics, like, temperature, entropy and the Bejan number, in the constricted region with the help of graphs. Figure 1 illustrates the effect of EP material parameter B on velocity profile. It shows decreasing behavior in the velocity as B increases. Figures 2 and 3 depict a 3-D view of temperature profile for parabolic and irregular stenotic channel, respectively. It can be seen that temperature attains highest value in the narrow part as compared to the wider part and this happened due to the increased convection process when fluid enters in the narrow part. When fluid enters in the narrow part its velocity increases which helps in augmenting the convection process. This behavior could be seen from figs. 4 and 5 (for both parabolic and irregular stenosis cases) where velocity is shown to be maximum in the constricted region. Figure 6 shows the contour graph of isotherms for parabolic and irregular shapes of stenosis. It is quite clear from the figure that temperature is maximum in the narrow part of the constriction and near to the lower heated wall of the channel for both cases.

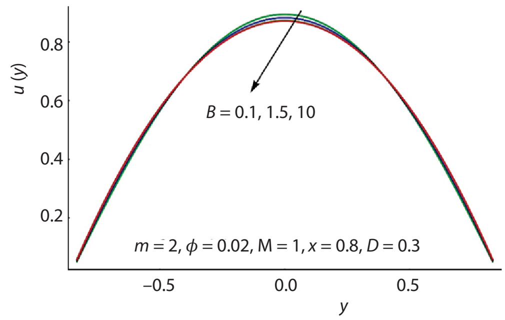

Figure 1. Effect of varying material parameter *B* on the velocity profile

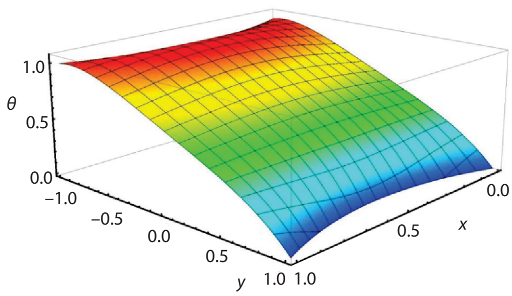

Figure 2. A 3-D view of temperature profile when Br = 1, M = 1, *B* = 0.5, *D* = 0.05, *δ* = 0.2, and *m* = 2

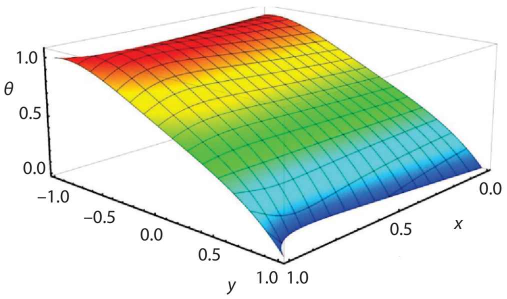

Figure 3. A 3-D view of temperature profile when Br = 1, M =1, *B* = 0.5, *D* =0.05, *δ* = 0.2, and *m* = 11

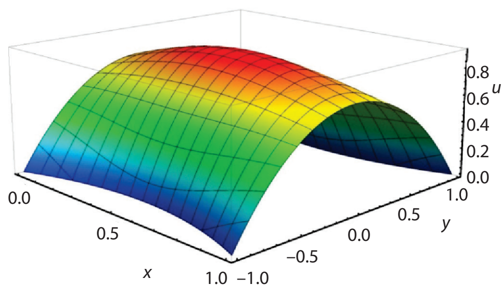

Figure 4. A 3-D view of velocity when Br = 1, M = 1, *B* = 0.5, *D* = 0.05, *δ* = 0.2, and *m* = 2

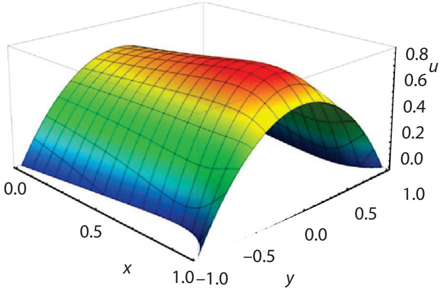

Figure 5. A 3-D view of velocity when Br = 1, M = 1, *B* = 0.5, *D* = 0.05, *δ* = 0.2, and *m* = 2

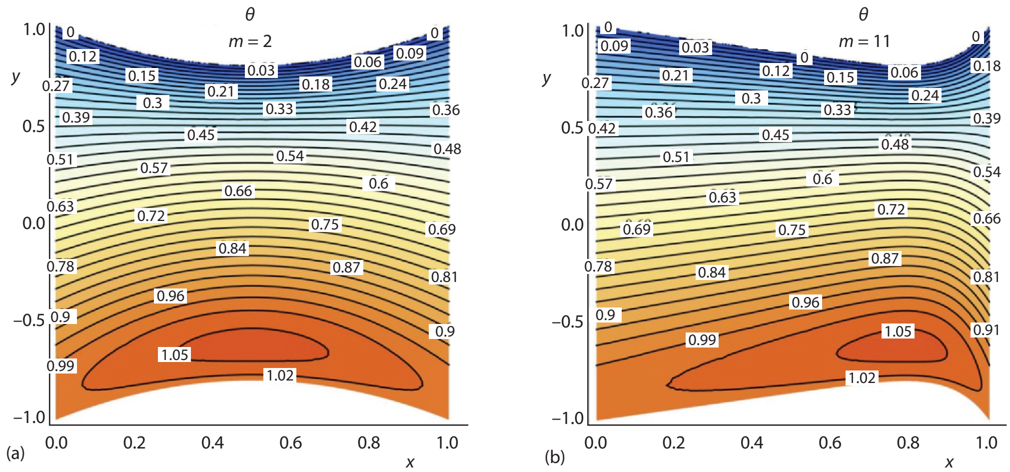

Figure 6. Isotherm lines for regular shape; (a) and irregular shape, (b) stenosis

Figures 7 and 8 reflect a 3-D glimpse of entropy generation, N_G, for the two different shapes, parabolic (m = 2) and irregular (m = 11). The figures show that the entropy production is maximum at the narrow region of the channel and reduces in the wider parts. Moreover, entropy generation is maximum near the walls and is minimum at the center of the channel. To disclose the fact that which kind of shape of stenosis gives highest rate of entropy production we plotted fig. 9. It is observed from the figure that the entropy generation takes its highest value for parabolic shape (m = 2) and it decreases as the shape parameter takes larger values (irregular stenosis). It is also observed that variations in entropy are more noticeable at the channel boundaries rather than the channel center. Same behavior of entropy production is depicted in fig. 10 which displays

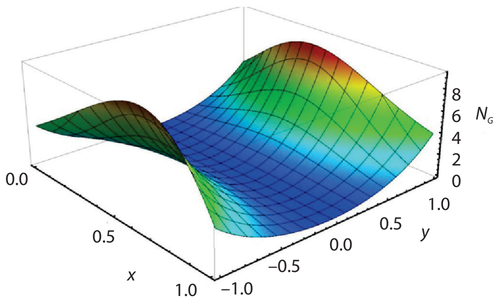

Figure 7. A 3-D view of N_G when *α* = 0.2, Br = 1, M = 1, *B* = 0.5, *D* = 0.05, *δ* = 0.2, and *m* = 2

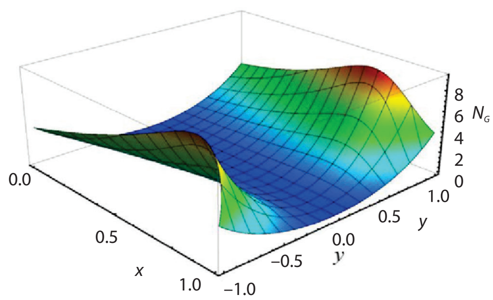

Figure 8. A 3-D view of N_G when *α* = 0.2, Br = 1, M = 1, *B* = 0.5, *D* = 0.05, *δ* = 0.2, and *m* = 11

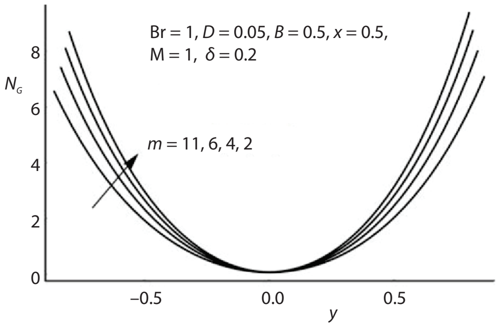

Figure 9. Effect of m on entropy generation number N_G

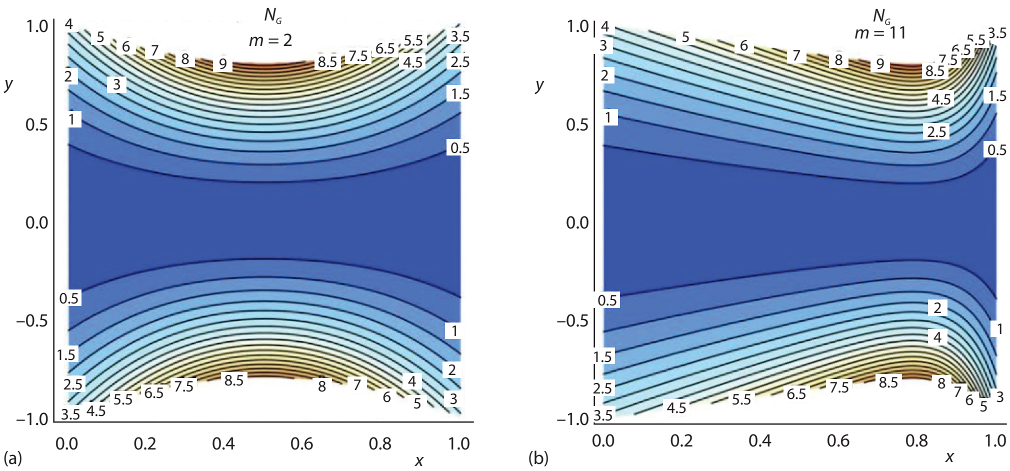

Figure 10. Entropy lines when α = 0.2, Br = 1, M = 1, B = 0.5, D = 0.05, δ = 0.2

contour lines of entropy generation rate for parabolic shape 10(a) and irregular shape 10(b) at $m = 2$ and $m = 11$, respectively. From fig. 11, it can be examined that N_G increases with an increase in EP parameter, B, however, the effect of B is dominant in boundaries and negligible at the center of the channel. To see the discriminating effects of heat transfer and fluid friction irreversibilities we plotted the Bejan number in fig. 12. It shows that heat transfer irreversibility is dominant in the center of the channel while the fluid friction irreversibility dominates near-walls. Moreover, as parameter B increases fluid frictional irreversibility increases. This is due to the strong shear stress at larger values of EP constant.

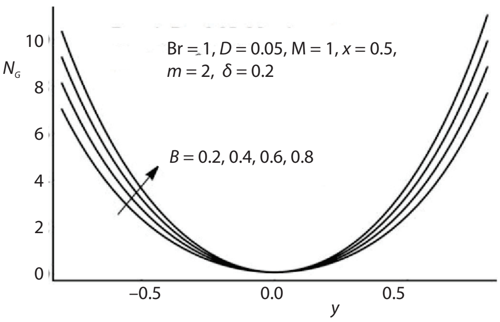

Figure 11. Effect of parameter B on entropy generation number N_G

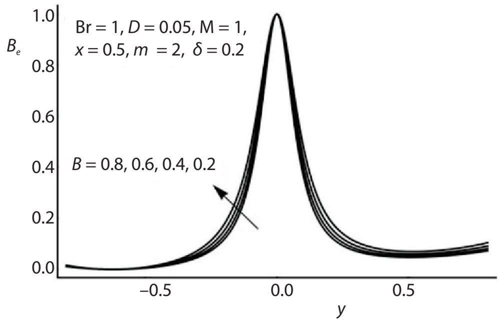

Figure 12. Effect of B on Bejan number

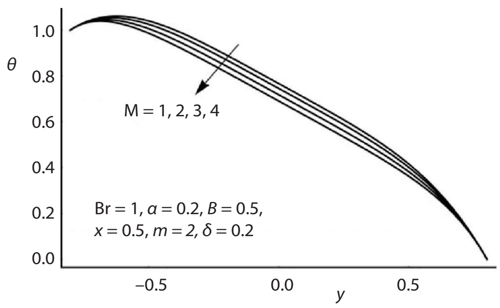

Figure 13. Effects of M on temperature, θ

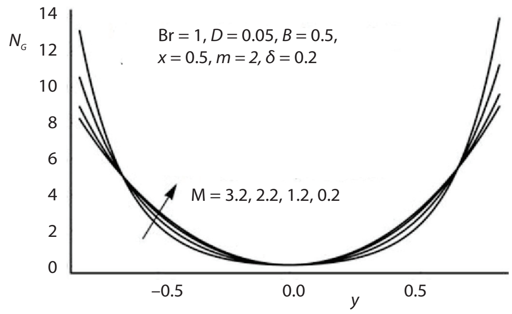

Figure 14. Effect of M on entropy generation number N_G

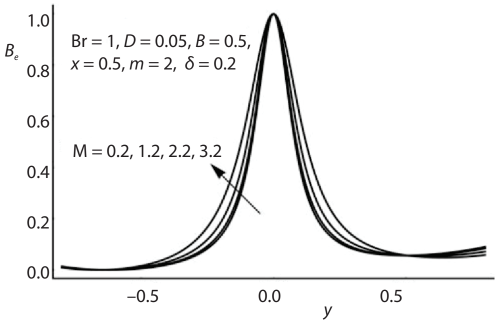

Figure 15. Effect of *M* on Bejan number

Figure 13 shows the temperature, θ, decreases as the Hartmann number, increases. Such type of behavior is seen due to lower flow rate at higher magnetic field for which convection phenomenon becomes slow. Figure 14 portrays that as the Hartmann number increases the entropy generation number N_G increases near the channel walls and then a point of inflection occurs at mid-half of the channel after which N_G decreases. The same behavior is seen at the upper half part of the channel. To examine the comparative effects of the heat transfer and fluid friction irreversibilities the Bejan number is plotted in fig. 15 for variations in the Hartmann number. From the figure it is found that heat transfer irreversibility rises as the magnetic field increases. Such type of outcome is quite expected since large Hartmann number contributes in lowering the fluid temperature and increasing the temperature differences which results in rise of heat transfer irreversibility.

Conclusions

In this article a complete thermodynamical analysis has been made for the convective heat transfer of EP fluid-flow through a constricted channel in the presence of magnetic field effect. The main objective is to discuss the entropy production in a stenotic channel having different structures of stenosis. We conclude the following results.

- The temperature and velocity are maximum in the narrow regions of the channel for both parabolic and irregular shapes of stenosis.
- The entropy production is maximum in the narrow part of channel and decreases in the wider part.
- The parabolic shape of stenosis causes larger entropy production as compared to the irregular shapes.
- The EP material constant *B* also produces entropy and the fluid friction entropy augments as this constant increase.
- The magnetic field helps in increasing the heat transfer irreversibility.

Acknowledgment

The authors would like to acknowledge the financial support provided by the Deanship of Research Development, Prince Mohammad Bin Fahd University Al-Khobar.

Nomenclature

a – stenosis location, [m]
b – stenosis length, [m]
B – dimensionless EP material parameter
Be – Bejan number
Br – Brinkman number
B_0 – applied magnetic field, [T]
c_0 – reference velocity, [ms^{-1}]
C^* – EP time scale parameter (s^{-1})
C_p – specific heat capacity, [JK^{-1}]
D – dimensionless EP material parameter
d_0 – channel width without stenosis, [m]
h – dimensionless stenosis height
h' – channel width with stenosis, [m]
k – thermal conductivity, [Wm^{-1}K^{-1}]
M – Hartmann number
m – shape parameter
Ns_{avg} – average entropy number
N_G – entropy generation number
p – dimensionless pressure
p' – fluid pressure, [Nm^{-2}]
S'''_{gen} – volumetric rate of entropy, [JK^{-1}]
S_{G0} – characteristic entropy, [JK^{-1}]
T – temperature field, [K]
T_1 – lower wall temperature, [K]
T_2 – upper wall temperature, [K]
u – dimensionless velocity component
u' – velocity component along wall, [ms^{-1}]
v – dimensionless velocity component
v' – velocity component normal to wall
x' – independent variable along wall, [m]
y' – independent variable normal to wall, [m]
x, y – dimensionless independent variables
$\forall$ – area of integrated region, [m^2]

Greek symbols

α – dimensionless temperature difference
β – EP material constant, [m^{2}N^{-1}]
δ' – maximum height of stenosis, [m]
θ – dimensionless temperature field
μ – dynamic viscosity, [kgm^{-1}s^{-1}]
ρ – density of fluid, [kgm^{-3}]
σ – electrical conductivity, [Sm^{-1}]
$\boldsymbol{\tau}$ – EP shear stress tensor, [Nm^{-2}]
ϕ – amplitude ratio
$\forall$ – area of integrated region, [m^2]

References

[1] Shukla, J. B., *et al.*, Effects of Stenosis on Non-Newtonian Flow of the Blood in an Artery, *Bulletin of Mathematical Biology*, *42* (1980), 3, pp. 283-294
[2] Haldar, K., Oscillatory Flow of Blood in a Stenosed Artery, *Bulletin of Mathematical Biology*, *49* (1987), 3, pp. 279-287
[3] Makinde, O. D., Alagoa, K. D., Effect of Magnetic Field on Steady Flow through an Indented Channel, AMSE Modelling, *Measurement and Control B*, *68* (1999), 1, pp. 25-32
[4] [4] Mekheimer, K. S., Kot, M. A. E., The micropolar fluid model for blood flow through a tapered artery with a stenosis, *Acta Mechanica Sinica*, *24* (2008), 6, pp. 637-644
[5] Tripathi, D., A Mathematical Study on Three Layered Oscillatory Blood Flow Through Stenosed Arteries, *Journal of Bionic Engineering*, *9* (2012), 1, pp. 119-131
[6] Sud, V. K., *et al.*, Pumping Action on Blood by a Magnetic Field, *Bulletin of Mathematical Biology*, *39* (1977), 3, pp. 385-390
[7] Mekheimer, K. S., El Kot, M. A., Influence of Magnetic Field and Hall Currents on Blood Flow through a Stenotic Artery, *Applied Mathematics and Mechanics-English Edition*, *29* (2008), 8, pp. 1093-1104
[8] Kumar, S., *et al.*, Oscillatory MHD Flow of Blood through an Artery with Mild Stenosis, *IJE Transactions A: Basics*, *22* (2009), 2, pp. 125-130
[9] Bejan, A., A Study of Entropy Generation in Fundamental Convective Heat Transfer, *Journal of Heat Transfer-Transactions of the ASME*, *101* (1979), 4, pp. 718-725
[10] Bejan, A., Second Law Analysis in Heat Transfer, *Energy*, *5* (1980), 8-9, pp. 720-732
[11] Bejan, A., *Entropy Generation Minimization*, CRC Press, Boca Raton, New York, USA, 1996
[12] Adesanya, S. O., Makinde, O. D., Thermodynamic Analysis for a Third Grade Fluid through a Vertical Channel with Internal Heat Generation, *Journal of Hydrodynamics, Ser. B*, *27* (2015), 2, pp. 264-272
[13] Munawar, S., *et al.*, Thermal Analysis of the Flow over an Oscillatory Stretching Cylinder, *Physica Scripta, 86* (2012), 6, 065401
[14] Butt, A. S., *et al.*, Slip Effects on Entropy Generation in MHD Flow over a Stretching Surface in the Presence of Thermal Radiation, *International Journal of Exergy*, *13* (2013), 1, pp. 1-20
[15] Ijaz, S., *et al.*, Entropy Generation Minimisation in a Moving Porous Pipe under Magnetic Field Effect, *International Journal of Exergy*, *26* (2018), 4, pp. 418-434
[16] Mahmud, S., Fraser, R. A., The Second Law Analysis in Fundamental Convective Heat Transfer Problems, *International Journal of Thermal Sciences*, *42* (2003), 2, pp. 177-186

[17] Butt, A. S., *et al*., Entropy Generation in the Blasius Flow under Thermal Radiation, *Physica Scripta*, *85* (2012), 3, p. 6, 035008
[18] Tasnim, S. H., *et al.*, Entropy Generation in a Porous Channel with Hydromagnetic Effect, *Exergy*, *An International Journal*, *2* (2002), 4, pp. 300-308
[19] Mehmood, A., *et al*., Entropy Analysis in Moving Wavy Surface Boundary-Layer, *Thermal Science*, *23* (2019), 1, pp. 233-241
[20] Souidi, F., *et al.*, Entropy Generation Rate for a Peristaltic Pump, *Journal of Non-Equilibrium Thermodynamics*, *34* (2009), 2, pp. 171-194
[21] Munawar, S., *et al*., Second Law Analysis in the Peristaltic Flow of Variable Viscosity Fluid, *International Journal of Exergy*, *20* (2016), 2, pp. 170-185
[22] Powell, R. E., Eyring, H., Mechanisms for the Relaxation Theory of Viscosity, *Nature*, *154* (1944), p. 427
[23] Yoon, H. K., Ghajar, A. J., A Note on the Powell-Eyring Fluid Model, *International Communications in Heat and Mass Transfer*, *14* (1987), 4, pp. 381-390
[24] Hayat, T., *et al*., Magnetohydrodynamic Flow of Powell-Eyring Fluid by a Stretching Cylinder with Newtonian Heating, *Thermal Science*, *22* (2018), 1, pp. 371-382
[25] Mahanthesh, B., *et al*., Unsteady 3-D MHD Flow of a Nano Eyring-Powell Fluid Past a Convectively Heated Stretching Sheet in the Presence of Thermal Radiation, Viscous Dissipation and Joule Heating, *Journal of the Association of Arab Universities for Basic and Applied Sciences*, *23* (2017), June, pp. 75-84
[26] Siddiqui, A. A., *et al*., Influence of the Magnetic Field on Merging Flow of the Powell-Eyring Fluids: An Exact Solution, *Meccanica*, *53* (2018), 9, pp. 2287-2298
[27] Khan, S. U., *et al*., Soret and Dufour Effects on Hydromagnetic-Flow of Eyring-Powell Fluid over Oscillatory Stretching Surface with Heat Generation/Absorption and Chemical Reaction, *Thermal Science*, *22* (2018), 1, pp. 533-543
[28] Saleem, N., Munawar, S., A Mathematical Analysis of MHD Blood Flow of Eyring-Powell Fluid through a Constricted Artery, *International Journal of Biomathematics*, *9* (2016), 2, 1650027

Paper submitted: January 25, 2018
Paper revised: September 21, 2019
Paper accepted: October 25, 2019

© 2020 Society of Thermal Engineers of Serbia
Published by the Vinča Institute of Nuclear Sciences, Belgrade, Serbia.
This is an open access article distributed under the CC BY-NC-ND 4.0 terms and conditions